Some of the PMTs are dead by short circuit or some other unknown response. The time variation in the number of dead PMTs is shown figure 3.14. The fraction of the dead PMTs is about 1.4%.

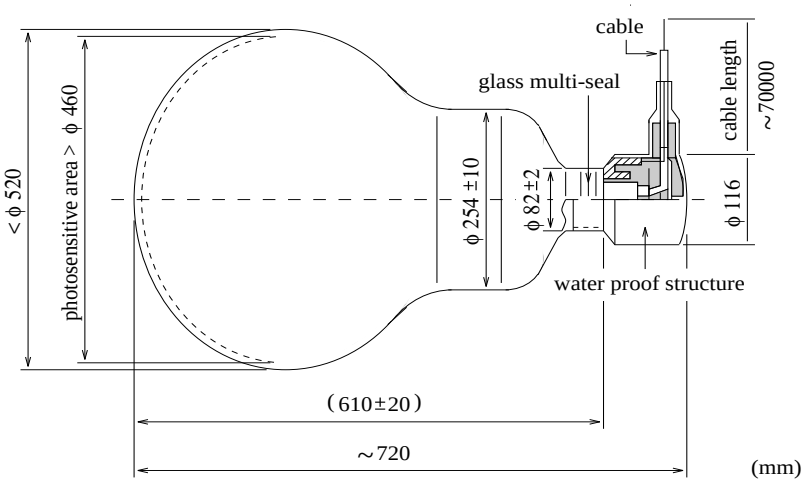

Figure 3.10: Schematic view of a 50 cm photomultipiler tube (HAMAMATSU R3600-05).

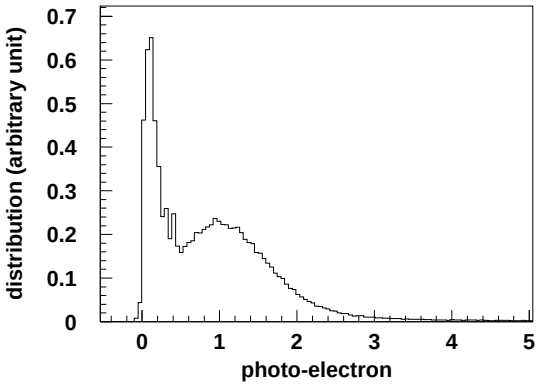

Figure 3.11: The single p.e. distribution from 50 m PMTs. There is a clear peak around 1 p.e.. A spike near the lowest region is caused by photo-electron that miss the first dynode.

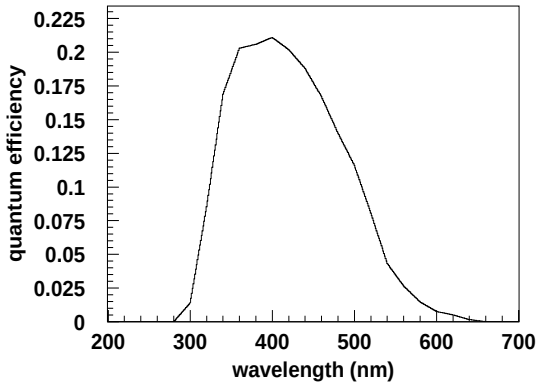

Figure 3.12: The quantum efficiency of the PMTs and the relative *Čerenkov* spectrum as a function of light wavelength.

Figure 3.15 shows the time variation of high and low energy trigger rate from the beginning of SK-I in ID detector. The right plot is high energy trigger rate and the left plot is low energy trigger rate.

3.4 The water purification system

In purities in the SK water can cause strong attenuation and scattering of *Čerenkov* light. Moreover, if they are radioactive, like ^{222}Rn and ^{220}Rn, they could become a possible source of background to the solar neutrino events, because the β-decay of their daughter nucleus causes a

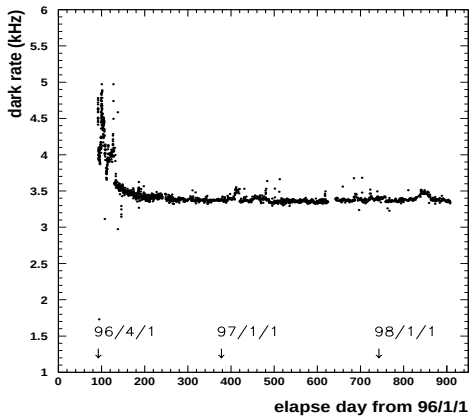

Figure 3.13: The time variation of dark rate from the beginning of SK.

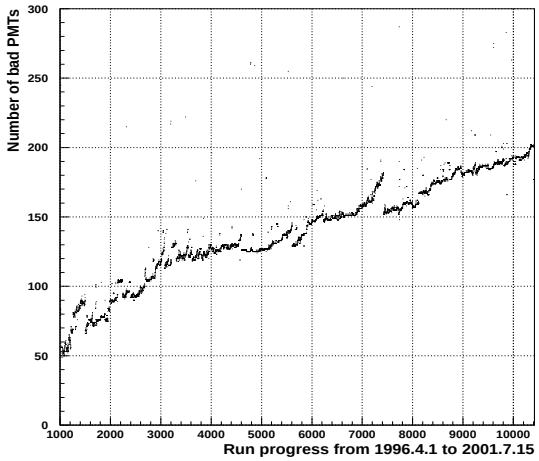

Figure 3.14: The time variation of the number of dead PMTs from the beginning of SK.

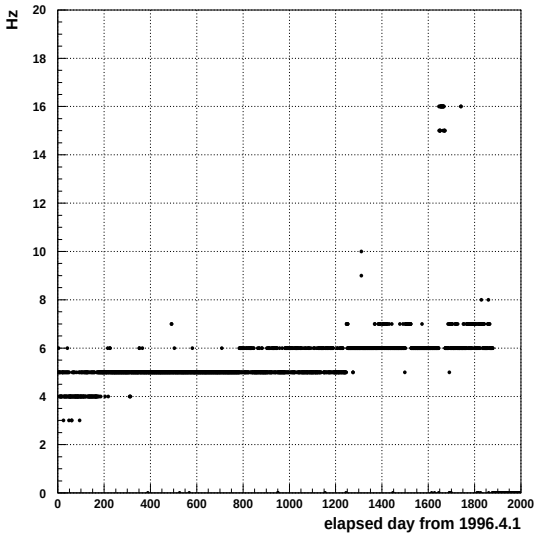

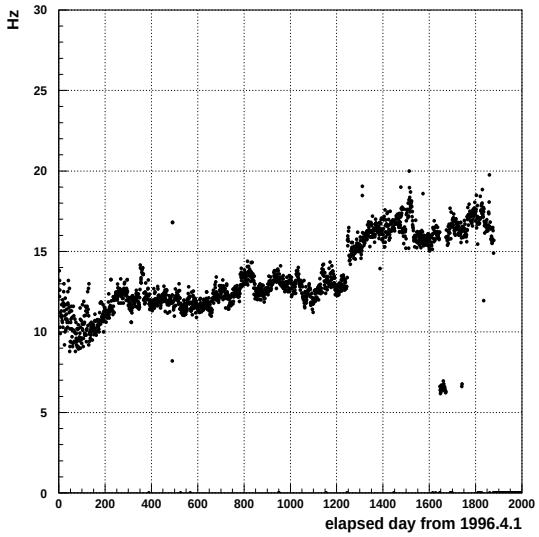

Figure 3.15: The time variation of high and low energy trigger rate from the beginning of SK.

similar event as solar neutrino event which means $\nu_e - e$ elastic scattering. The decay chain of ^{222}Rn is shown in figure 3.20. None of the electrons or γ rays from the decay chain have energy above threshold for this analysis 4.5 MeV. However, because of finite energy resolution of SK, such low energy electrons are sometimes observed as electrons with energy above 4.5 MeV. So, the purity of the water is essential for solar neutrino observation in SK.

The SK water purification system has been modified and upgraded with Organo Corporation. In this section, the basic components of the system is explained. The details of the modification and upgrading of the water system is explained in chapter 7 in detail.

The source of water in SK is an underground aquifer in the Kamiokande mine. The water purification system makes highly purified water from the mine water. Figure 3.16 is a basic schematic view of the water purification system. The water passes through the following components:

- 1 μm normal filter :
  Remove relatively large particles. Some of Rn also rejected with dust.

- Heat exchanger(HEX) :
  Water pumps increase the water temperature. The heat exchanger decrease the temperature down to about 12$\sim$13°C to inhibit bacterial growth and to suppress the water convection in the SK tank.

- Ion exchanger(IEX) :
  Removes metal ion ($Fe^{2+}, Ni^{2+}, Co^{2+}$) impurities in the water. It can also remove ^{218}Po which is a daughter nucleus as a result of the decay of ^{222}Rn and easily ionize. The water resistance is best indication of the concentration of the ion in the water. If no ion is in the water, the water resistance will be expected 18.2 MΩ. In the SK water, the water resistance is 17.9$\sim$18.2 MΩ.

- UV sterizer(UV) :
  To kill bacteria. The documentation states the number of bacteria can be reduced to less than $10^3 \sim 10^4$/100ml.

- Rn-less-air dissolving system :
  Dissolve Rn less air in water to improve the Rn removal efficiency of the vacuum de-gasifier.

- Reverse Osmosis filters (RO) :
  Reverse osmosis by a high performance membrane which removes even organisms on the other of 100 modular weight. The output water is put back into the mine stream. The dissolving oxygen in the out put water is 10.8 μg/L after VD.

- Vacuum De-gasifier (VD) :
  Removes gases (Rn, Oxygen, etc) dissolved in water; about 96% of the dissolved radon gas is removed at this stage.

- Cartridge Polisher (CP) :
  High performance ion exchangers using high quality ion exchanger material.

- Ultra Filter (UF) :
  Removes sub-μm contamination. After the Ultra filter, the water is returned to the detector. The UF removes 10% of the water passed through. That water is recirculated through the water purification system again via the following equipment, which is shown by the dashed line in the figure.

- Membrane Degasifier (MD) :
  A membrane degasifier (MD) also removes radon dissolved in water. It is made of 30 hollow fiber membrane modules and a vacuum pump. A flow rate of 30 L/min of Rn-less

air from the air purification system is supplied to the MD system as purge gas. The typical pressure in the MD system is 2.6 kPa. The typical concentration of dissolved oxygen after the MD is 0.3 mg/L. The measured removal efficiency for radon is about 83%.

Usually, the water purification system supplies the purified water from the bottom of the tank and removes it from the top of the tank. The maximum capacity of the flow rate is 70 ton/hour. usually, the flow rate is 35 ton/hour. A summary of the quality of the purified water is given in table 3.3.

Impurities	Reduction efficiency
^{222}Rn	~99%
O_2	~96%
Dust $> 0.1\mu$m	~99.7%
Bacteria	~100%
Ion	~99%

Table 3.3: The summary of the quality of the purified water.

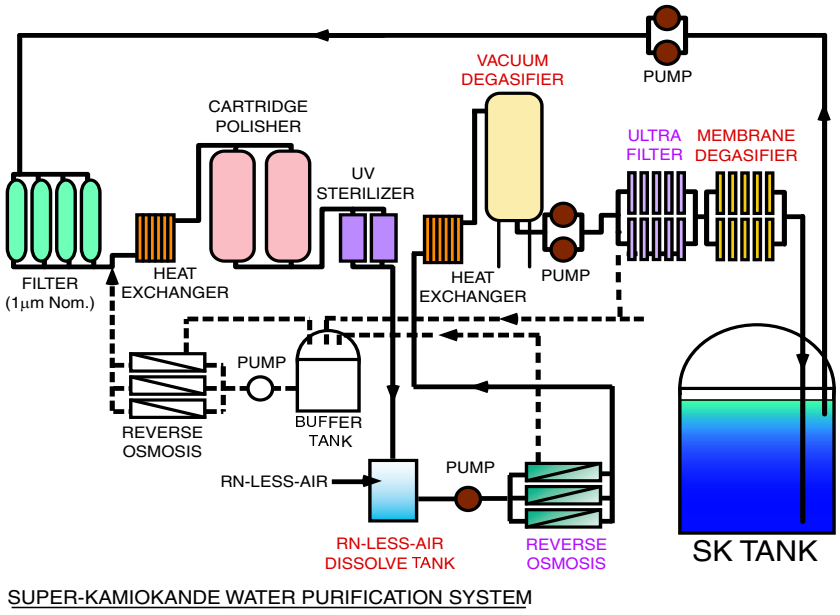

Figure 3.16: A schematic view of the water purification system.

3.5 The air purification system

SK is situated in mine, and the ^{222}Rn concentration in the mine air is 50~2000 mBq/m^3. Therefore the detector is literally surrounded by the source of Rn gas. The rock dome above the water tank and the hallway are covered with Mineguard polyurethane material, which prevents Rn gas emanation from rocks. Double doors at all entrances also limit the amount of mine air that entries the detector area.

To keep radon levels in the dome area and water purification system below 100 Bq/m^3, fresh air is continuously pumped at approximately 10 m^3/min from outside the mine through an air duct along 1.8 km Atotsu tunnel to the experimental area. This flow rate generates a slight

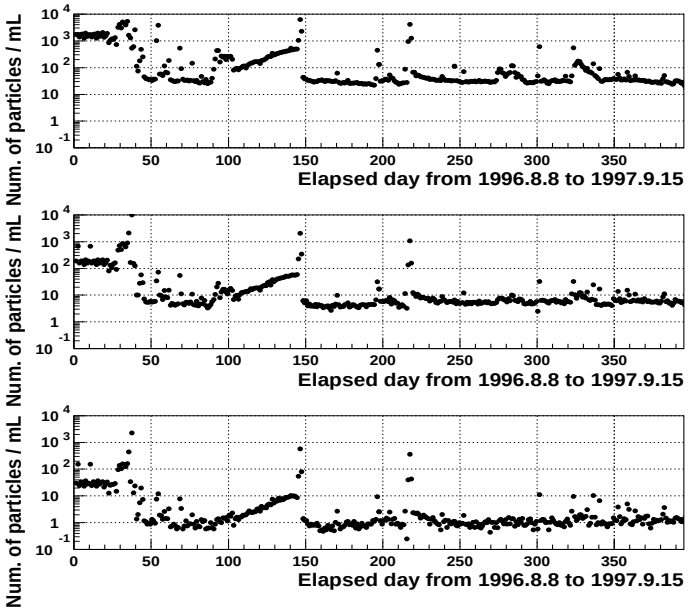

Figure 3.17: The time variation of the number of particles in the purified water. Each figure shows the number of particles of 0.1,0.2, and 0.3 μ size respectively from the top figure.

over-pressure in the SK experimental area, minimizing the entry of ambient mine air. A "Radon hut" in figure 3.7 was constructed near the Atotsu tunnel entrance to house equipment for the dome air system : a 40 hp air pump with 10 m^3/min/15 PSI pump capacity, air dehumidifier, carbon filter tanks, and control electronics. Fresh air from an intake (initially located at the Radon hut) is fed in to the air pump, and is then pumped through a dehumidifier, a carbon filter tank, and finally through a 1.8 km air duct from the Atotsu entrance to the experimental area. An extended intake pipe was installed at a location approximately 25 m above Atotsu tunnel entrance, where radon level concentration was found to remain at 10$\sim$30 Bq/m^3 all year long. Thus the 10 m^3/min fresh air flow from the Radon hut keeps the radon levels in the experimental area at approximately 30$\sim$50 Bq/m^3 throughout the year.

A part of the fresh air from the Radon hut is purified to Rn-less air with the air purification system. Figure 3.18 is a schematic view of the air purification system. It consists of three compressors, a buffer tank, driers, filters, and activated charcoal filters. The components of the air purification system as follows:

- Compressor : Takes in air from outside the mine and pressurizes it 7$\sim$8.5 atom.
- 0.3,0.1,0.01 μm filter : Removes dust in air.
- Air drier : Absorbs moisture since the radon reduction efficiency of the carbon column dependents on the humidity air.
- Carbon column (8 m^3): CO (Activated charcoal) absorbs Rn.
- Active charcoal (50 L) : Active charcoal cooled to -41°C traps the Rn.

Finally, after the air purification system, Rn reduction efficiency is $\sim$99.98% [1]. Figure 3.21 and figure 3.22 are the time variations of the radon concentration in various air.

Rn-less air is mainly supplied to $\sim$60 cm gap between the water surface and the top of the Super-Kamiokande tank. The Rn-less air is kept at a slight overpressure to help prevent ambient radon-laden air from entering the detector. Typical flow rates, dew point, and residual radon concentration are 18 m^3/hour, $\sim$-80(+1 kg/cm^2)°C, and a few mBq/m^3, respectively.

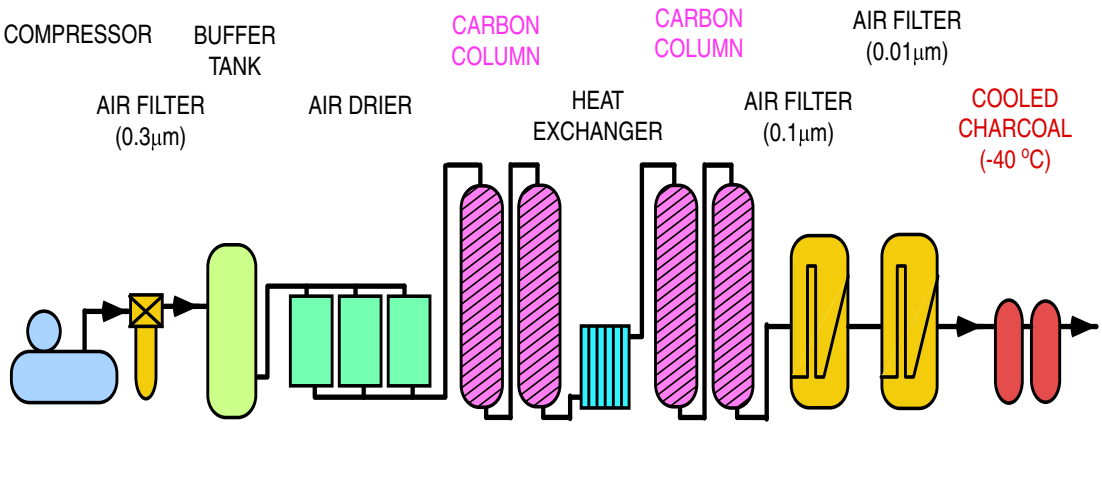

Figure 3.18: A schematic view of the air purification system.

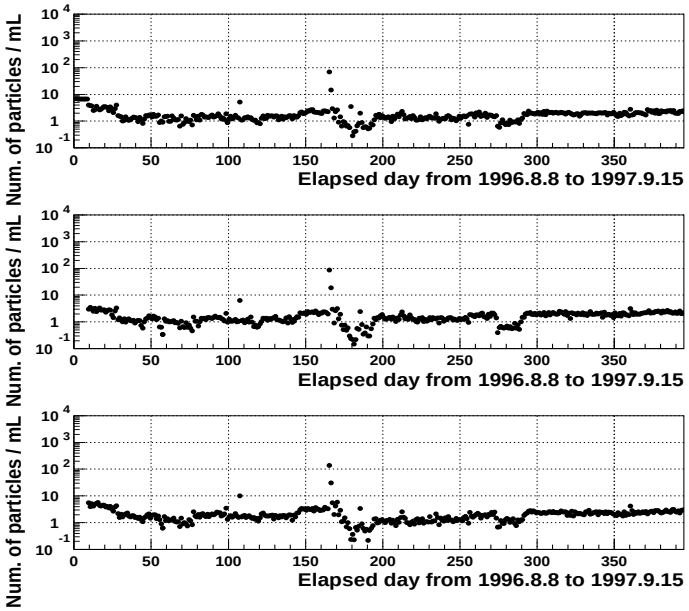

Figure 3.19: The time variation of the number of particles in the purified air. Each figure shows the number of particle of 0.1,0.2, and 0.3 μ size respectively from the top figure.

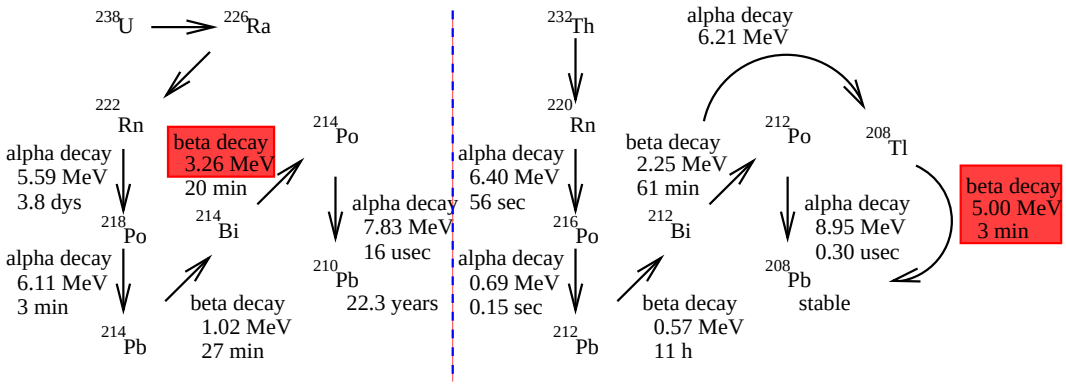

Figure 3.20: Rn decay series. The left side shows Uranium series of Rn. The right side shows Thorium series of Rn.

Table 3.4 is the summary of the radon concentration in the various samples. Table 3.5 is the list of the temperature condition at the various points.

Standard Samples	Rn concentration(Bq/m^3)
Fresh air	0.5∼1.0
Air in the underground	1.0×10^3∼4.0×10^6
Water in the underground	3.0×10^3∼4.0×10^7
Kamioka Samples	**Rn concentration(Bq/m^3)**
Air in the mine	winter 8.0×10^1∼1.0×10^2
	summer 6.0×10^3∼1.0×10^4
Dome air on the tank	5×10^1∼6.0×10^1
Purified air after the system	3.0×10^{-3}∼4.0×10^{-3}
Purified air in the tank gap	1.0×10^{-2}∼2.0×10^{-2}
Purified water after the system	6.0×10^{-3}∼10.0×10^{-3} (before upgrade)
	$<1.0\times10^{-3}$ (after upgrade)
Purified water in the SK tank	$\sim5.0\times10^{-3}$ (before upgrade)
	1.0×10^{-3}∼2.0×10^{-3} (after upgrade)
Return water from the SK tank	1.0×10^{-2}∼1.5×10^{-2} (before upgrade)
	$<2.0\times10^{-3}$ (after upgrade)

Table 3.4: The summary of the Rn concentration. Before and after mean before water system upgrading and after water system upgrading respectively.

3.6 The data acquisition system

3.6.1 The inner detector system

An overview of the data acquisition (DAQ) system is shown in figure 3.23. The signal cables which come from PMTs of ID and OD are extended on the top of the tank, where the electronics systems are located. The ID PMT signal cables (70m) are fed into ATM (Analog Timing Module) modules in a TKO (Tristan-KEK-Online) system. A TKO crate contains a GONG module (GO or NoGO, which distributes control signals as a master module to its slave modules), a SCH module (Super Controller Header, which is a bus-interface module between TKO and VME (Versa Module Europe)), and 20 ATM modules (which digitize analog signals from PMTs for

Chapter 7

The approaches to radon reduction

The radioactivity from radon (Rn) in pure water is a major background for observing solar neutrinos at SK. After the data reduction, the Rn background is remaining in the data. Since the Rn events behave as solar events, it is difficult to reduce the Rn events by analysis tool.

Figure 7.1 shows the $\cos\theta_{sun}$ distribution for each energy thresholds in low energy region. The excess to solar direction indicates observed solar events. The flat contents for the excess to solar direction indicates Rn dominant background. As a energy threshold is lowered, the obtained peak to solar direction becomes smaller. Then, the Signal(excess)/Noise(flat) ratio becomes wrong.

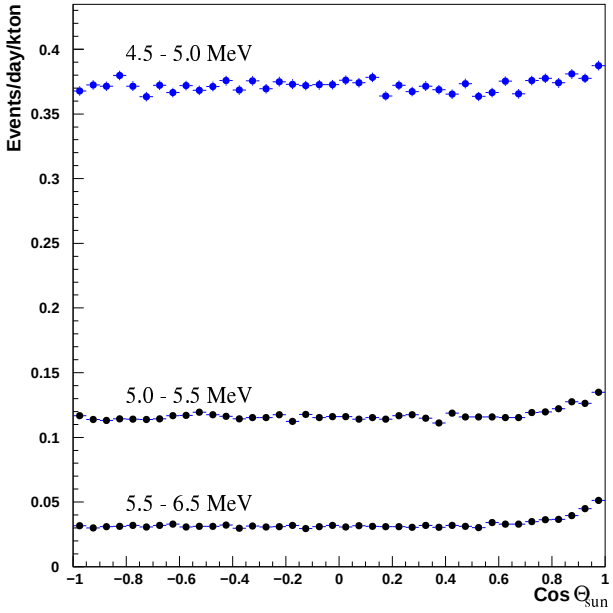

Figure 7.1: The $\cos\theta_{sun}$ distribution for each energy thresholds in low energy region.

Therefore, we have made an effort to reduce the Rn in pure water, physically, in order to observe low energy solar neutrino flux.

In this chapter, the following Rn reduction approach is described.

- The radon source in the SK water purification system was investigated and improved in Dec 2000.
- We have also studied the possibility of the Membrane Degasifier as the new radon reduction system. It was installed in the water system in February 2001.

By water system improvements, the radon concentration in the SK supply water was decreased by a factor of about 5. Basing on this result, the SK low-energy event rate analysis

concluded that the current main source of the radon background is the emanation from the PMT glass, and convection is the main driving force for transporting the radon in the detector. At the last of this chapter, the current status of the radon background reduction and the future prospects are presented.

7.1 Solar neutrinos in Super-Kamiokande

An important task of the SK detector is to measure the energy spectrum of the recoil electrons from ^{8}B and rare HEP solar neutrinos [5].

The energy spectrum of solar neutrino is distributed from 0 MeV up to 20 MeV. However the current analysis energy threshold is 5.0 MeV in the total recoil electron energy [5]. It is desirable to discuss the spectrums in the low-energy region in order to determine oscillation mechanism of the solar neutrinos. One of the important requirements of the solar neutrino observation in SK is to lower the energy threshold for the solar neutrino analysis as much as possible. The observation of the solar neutrino spectrums in the low-energy region is precluded by the remaining large background events after the event selection.

7.2 Radon background in the SK tank water

The analysis threshold is determined by the level of the background events and the event trigger threshold. The trigger threshold at 50% efficiency is 3.7 MeV and at 95% is 4.2 MeV. The dominant background sources in the low-energy region (E $\leq$ 6.5 MeV) are ^{222}Rn in the pure water, which cause a similar event to the solar neutrino events due to the beta decays of the radon daughters and external radioactivity such as gamma-rays from the PMT glass. After all reduction steps for the solar neutrino analysis, the S/N is approximately 1 above 5.0 MeV in the solar direction. It is supposed from SK low-energy events that the radon concentration in the SK tank is 2.0$\sim$3.0 mBq/m^3. In order to study the complete energy spectrum, it is desirable to lower the analysis energy threshold from 5.0 MeV to 4.5 MeV. This subject also means that the radon in pure water must be reduced as far as possible. For example, the radon concentration in the SK tank should be reduced down to less than 1.0 mBq/m^3.

For the SK detector, the following steps were done in order to achieve the needed radon reduction. Sufficient radon reduction for us means that we reduce the radon concentration in the SK supply water down to 1.0 mBq/m^3 which is not observed as low-energy events in the SK detector.

First of all, a super high sensitivity radon detector for water was developed to monitor the low radon concentration in the pure and degasified water before and after the radon reduction. The sensitivity of the developed radon detector is 0.7 (mBq/m^3)/day [102]. Secondly, the radon source was investigated in the SK water system by using the developed radon detector. Thirdly, we have also studied the utilization of the Membrane Degasifier (MD) as a more efficient radon reduction system. This new radon reduction system was also estimated by using the developed radon detector. After these steps, SK water system was improved. Finally, we concluded that the remaining background events in the low-energy region from 4.5 MeV to 6.5 MeV originated from the radon emanated from the glass of the PMTs in the SK detector.

7.3 The upgrades of water system in March 2000.

The total 50,000 tons of purified water in the SK is circulated through a water purification system with the flow rate of about 35 ton/hour in a closed system. The flow rate mode has started since July 1998. The water is circulated by the return pump which returns water from SK tank, and the supply pump which supplies water to the SK tank.

Figure 3.16 in chapter 3 shows a schematic view of the upgrading and improved SK water purification system in the final state of the SK-I. The SK water purification system has been improved and upgraded during the experiment basing on various studies.

In March 2000, some upgrading of the water purification system was done for following points in the figure 3.16.

First, the UF system was reinforced from 17 modules to 23 modules. Secondly, the RO system was also reinforced just before the VD system in addition to the existing RO system. These reinforcements make an effect on the removal of of the further dusts. Thirdly, the radon-free-air dissolve tank is installed before the VD system in order to increase radon removable efficiency at the VD system. In the VD system, 3600 L plastic balls like gyros were used to increase the surface area for vacuum degasification. The plastic balls were pointed out about the radon emanation from them. We actually measured the radon emanation from 100L balls of vinyl chloride and a stainless steel with an electro polished. The quality of the material was changed from a vinyl chloride to a stainless steel with an electro polished in a point of view of less radon emanation. We analyzed SK low-energy events from 4.5 MeV to 6.5 MeV before and after these upgrades. However, the effect of these upgrades was not observed.

Table 7.1 shows a summary of uranium and thorium concentration in each water. The concentration was measured with an ICP-MS device at the detection limit of 4.0 ppq. From the summary, we conclude that the SK supply water is super-high quality.

Measuring point	Uranium concentration	Thorium concentration
Mine water	3.0×10^5 ppq	32.0 ppq
SK supply water	0.2 ppq	0.4 ppq
SK return water	13.0 ppq	59.0 ppq

Table 7.1: A summary of Uranium/Thorium concentration in SK water.

7.4 Radon source search in the SK water purification system

First of all for radon background reduction, the radon source in the SK water purification system was investigated from Jun. 2000 to Sep. 2000 in order to reduce the radon background in the SK supply water physically. Figure 7.2 shows the flow chart of the SK water system.

In the figure 7.2, 'Point x' indicates a measuring point. We have measured the radon concentration between each components using the developed super high sensitivity radon detectors for water with 700L of collection volume (700L radon detector [102]). The radon is detected by electrostatic collection of the daughter nuclei of ^{222}Rn and the energy measurement of the alpha decay with a PIN photodiode. The sample water was taken from these measuring points using the water pump by the flow rate of 1.0 L/min. The water was forwarded to the radon detector and measured. The flow rate is set in the same way as the calibration. The detection efficiency, used as a calibration factor, of the 700L radon detector was measured by a standard radon water source and it is $14.6\pm1.5(stat.)^{+1.6}_{-1.5}(syst.)$ (counts/day)/(mBq/m^3). This value is larger than the previous 70L radon detector [101] by a factor of about five [102]. The detection limits which means three standard deviation in excess of the signal above the background of the radon detector for water, is 0.7 (mBq/m^3)/day in one-day measurement. The details about the super high sensitivity radon detectors are reported in reference [102]. This value is smaller than the 70L radon detector by a factor of about six. The radon detectors are connected to a workstation via a network, and they are monitored in real-time.

Table 7.2 and figure 7.3 (filled circles) shows the radon concentration at each components.

The results show that the radon concentration just after the IE is about a factor of 14 higher than that of the SK supply water. Even though the radon concentration just after the IE is

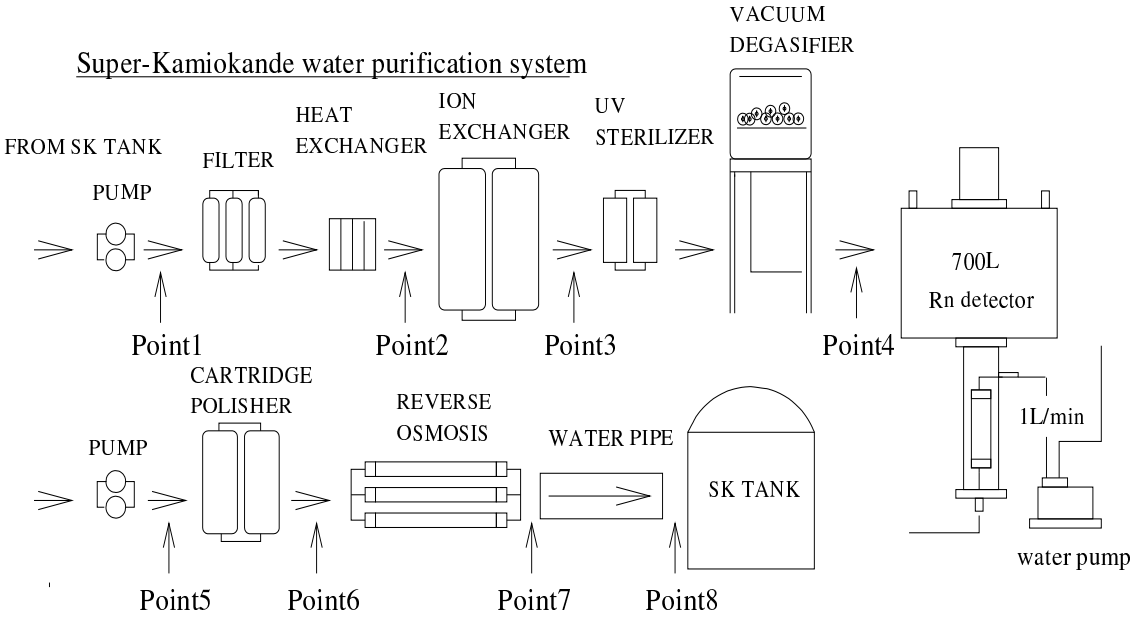

Figure 7.2: The flow chart of the SK water system and the search points of the radon source.

Measuring point	Component	radon concentration(mBq/m^3)
Point 1	after return pump	13.6±1.9
Point 2	just before IE	16.0±1.3
Point 3	just after IE	88.0±0.6
Point 4	just after VD	4.2±0.8
Point 5	just after supply pump	3.7±0.7
Point 6	just after CP	6.8±1.8
Point 7	just after UF	5.8±0.5
Point 8	just before the SK tank	6.5±0.2

Table 7.2: The radon concentration at each water system components. Error is statistical only.

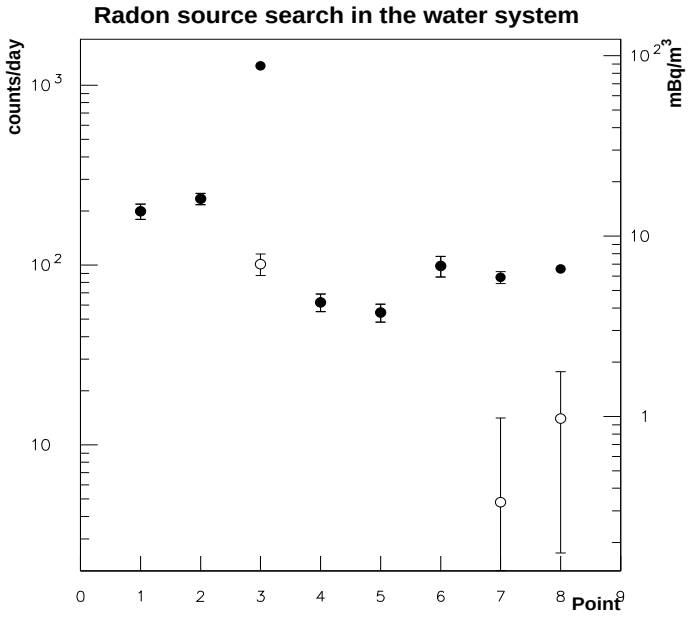

Figure 7.3: The radon concentration at each water system components. Error is *stat.* only. Points of the horizontal axis indicates component number. See table for component number.

so high, it was reduced by the VD system by a factor of about 20. This reduction efficiency (-95.0±1.0%) is almost the same level expected from the specification of the VD system.The CP produced about 46.0% of the radon concentration of the SK supply water comparing just before and just after CP system. From these results, we found two radon source points which are the IE system and CP system in the SK water purification system.

7.5 Membrane Degasifier as new radon reduction system

We studied the feasibility of the membrane degasifier (MD) from December 1999 to September 2000. The membrane degasifier is a hollow fiber with an outer diameter of 250 μm. The surface of this membrane has a structural feature wherein the inner surface has many small holes with a diameter of about 0.03 μm but no holes on the outer surface. The principle of the membrane degasifier is as follows. In the side separated with the membrane which let gas pass but water not pass (water phase), the water which contains gas flows. In the other side (gas phase), the pressure is reduced by the vacuum pump. Hence, the gas dissolved in the water pass through the membrane and transfered from water phase to gas phase.

In the case of the MD system installation in the SK water purification system, there are some requirements. The MD must be small, has a high radon reduction efficiency, and has a small radon emanation from itself. It is most important that radon emanation from membrane is small.

Before starting the test, we have compared the radon emanation from MD modules made by several companies and it was found that the one made by Dai-Nippon-Ink and Chemicals inc. gave the lowest radon emanation. The product is SEPAREL EF-040P. The radon concentration emanated from the membrane is 0.020±0.004(*stat.*) mBq/1module/day. Uranium and Thorium in the Poly-4Methyl-Penten1 is less than 1 ppb, a value which was estimated by the KAWATESTU TECHNOSEARCH inc. at the level of the detection limit. From these results, we have studied the radon reduction efficiency only using a Dai-Nippon-Ink module. Table 7.3 shows the specification of a membrane degasifier module(SEPAREL EF-040-P) which was studied for is the radon reduction efficiency.

This module is able to reduce gas dissolved in water down to less than 25 ppb (25 μg/L)

Contents	Specification
Material of membrane	Poly-4Methyl-Penten1
Material of housing	Vinyl chloride resin for super pure water
Bonding agent	Urethane and Epoxy resin
Endcap	Polysulfon
Size	180mmϕ×673mmL
Capacity of treatment(Max)	2[ton/hour]
Active surface of membrane	$\sim$40[m^2]
Weight	$\sim$10.0[kg]

Table 7.3: The specification of a membrane degasifier module(SEPAREL EF-040-P) whose the radon reduction efficiency was studied.

for a vacuum pressure of 20 torr and a flow rate of 2 ton/hr and water temperature of 25 degrees centigrade and air temperature of 20$\sim$30 degrees centigrade. However, this ability is basically for oxygen dissolved in the water. In this thesis, it is reported for the first time that the radon reduction efficiency of the MD module was estimated using the super high sensitivity radon detector. Moreover, it is very important that this estimation was done under the special condition where oxygen in the water is already degasified by -96%.

A small setup was constructed on the SK tank as shown in figure 7.4 in order to estimate the radon reduction efficiency of the MD module.

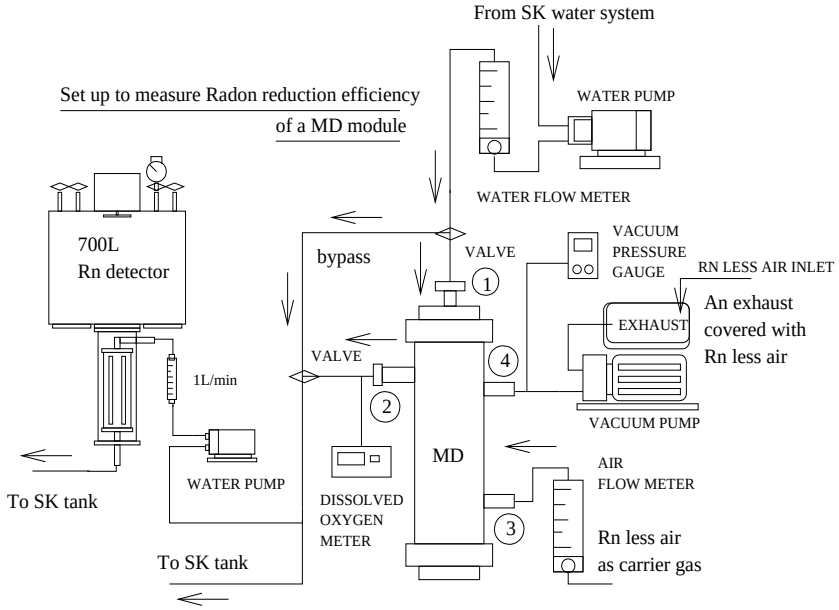

Figure 7.4: Setup to measure radon reduction efficiency of a MD module.

The setup consists of a MD module, two water pumps, a vacuum pump, a vacuum pressure gauge, a dissolving oxygen meter, and the 700L radon detector for water. In this setup, there are two routes of the water flow. In one route, the water passes through the MD module, In the other route, the water bypasses the MD module. When the radon concentration is measured by the former route, the run is called 'MD run'. The run is called 'SK water run' when the radon concentration is measured by the latter route. The water from the SK water purification system flows to one of the two routes by the manual selection. The flow rate was tuned by the flow rate meter from 0.2 tons/hour to 1.0 tons/hour. Then, a part of the water is forwarded to the radon detector to measure the radon concentration with a flow rate of 1.0 L/min and the left water is

forwarded to the SK detector.

In this MD module, the water flows the outside of the hollow fiber membrane and the inside of it is reduced the pressure by the vacuum pump. The water flows from No1 nozzle to No2 nozzle through the MD module in figure 7.4. We need to inject pure air to the vacuum phase in order to increase the radon reduction efficiency by the combining radon gas with air, because the water is already degasified. We used the radon-free-air as the carrier gas. The radon-free-air is produced by the SK air purification system, the details about it are reported in chapter 3. The carrier gas was injected from the No3 nozzle. The gas separated from the water was exhausted from the No4 nozzle by the vacuum pump. A noticeable point is that the exhaust of the vacuum pump was covered with the radon-free-air to prevent the open air from flowing into the MD from this exhaust.

In the figure, the data values and the data points were fit by using the following exponential function,

$$\mathrm{N}(T) = \mathrm{N}(0) \times \exp \frac{-\ln 2.0 \cdot T}{3.8} + \mathit{Constant} \tag{7.1}$$

where N(T) is the count rate at time T, N(0) is the obtained count rate at the injection time, and T is the elapsed time since the measurement starting in day. *Constant* indicates the value in the equilibration state of each of the measurements. We used this value in the case of the calculation of the radon reduction efficiency.

The efficiency depends on vacuum in the module, the flow rate of water through the module, and the amount of carrier gas flow into the vacuum phase of the module. We calculated the efficiency of the MD by comparing the radon concentration in 'SK water run' and it in 'MD run'. The formulation of the efficiency is given as :

$$\text{Efficiency} = \frac{\text{MD run[counts/day]-Background run[counts/day]}}{\text{SK water run[counts/day]-Background run[counts/day]}} \tag{7.2}$$

where the background run is estimated by stopping the water flow. Figure 7.5 shows a typical variation for the each runs, which are SK water run,background run, and MD run. A parenthesis(x/y) in the figure indicates a function of water(x) and carrier gas rates(y). In the figure, the MD effect was observed clearly for the SK supply water and the radon reduction succeeded almost down to the background level.

Table 7.4 shows a summary of the radon reduction efficiency of the MD module as a function of water and carrier gas. The error is statistical only.

Vacuum pressure(kPa)	Water flow (ton/hour)	Carrier gas (L/min)	radon reduction (%)	Dissolved oxygen(μg/L)
6.13	0.2	0.4	-93±4	525
8.50	0.2	1.0	-90±3	867
0.38	0.4	0.0	-83±3	5.6
0.35	1.0	0.0	-64±12	3.7
0.65	1.0	1.0	-83±5	235
0.93	1.0	2.0	-90±7	367

Table 7.4: A summary of the radon reduction efficiency of the MD module as a function of water and carrier gas. Error is statistical only.

It is possible that the MD module reduce radon by about 90% in the optimum condition although the water was already degasified by the -96% efficiency. In a point of view of the installation just before SK tank, the remarkable result is that the MD module is able to reduce radon by a factor of more than about 5 for the water flow rate about 1 ton/hour. A noticeable

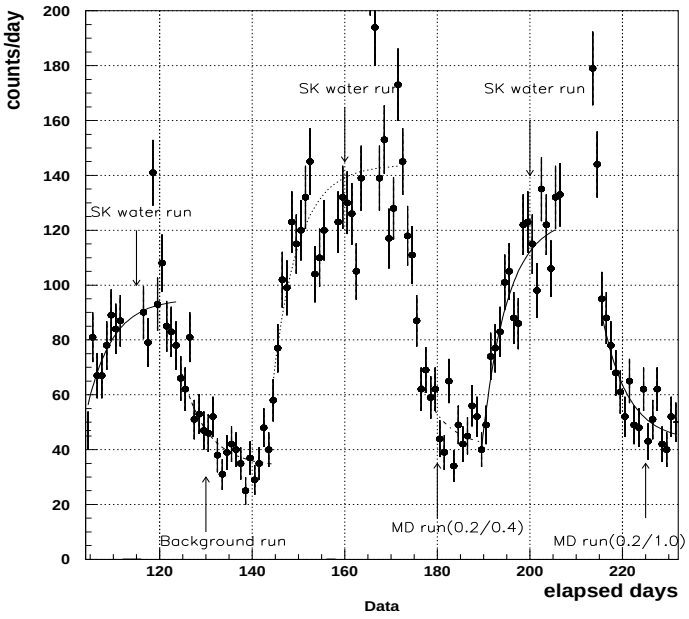

Figure 7.5: A typical variation for the each runs, which are SK water run,background run, and MD run. A parenthesis(x/y) in the figure indicates a function of water(x) and carrier gas rates(y).

point is that in this module test, the radon concentration of the SK supply water was 6.5±0.2 mBq/m^3 and the ability of the radon reduction was for the radon concentration in the water.

Considering a treatment of the amount of the SK supply water of 30 tons/hour, and an ability of the radon-free-air production, we decided to install a system with 30 MD modules between the water purification system and the SK tank as a final process of the SK supply water.

In the case of the installation, the optimum conditions are 1 ton/hour/module and the carrier gas of 1.0 L/min/module. A deserving special mention is that the exhaust of a vacuum pump was decided to be covered with radon-free-air because the phenomenon of the open air back-flow was observed in the experiment.

7.6 Improvements of water system in October 2000 and in February 2001

In the figure 3.16, the CP system and the MD system were the improvements based on the studies of the radon source search and the feasibility of the MD system.

In October 2000, improvements for the IE and the CP systems were done based on the results of the radon source search. First of all, we should explain the difference between IE and CP. Both have the functionality of removing ions. The main difference between them is that IE is re-generatable, but CP is not. The power to capture ions by IE is weaker than that of CP and that is why IE is re-generatable. When we get a "new" IE resin from the water system company, it is in most cases a re-generated one at the company. The company collected used IE resin from customers and re-generate them at once using a big plant. Hence, it is quite possible that even new IE resin has serious amount of Radium for us even though the resin is good enough for other customers. On the other hand, CP resin is made from raw materials and used only once. Therefore, it must have lower Radium concentration. The reason why we have been using both IE and CP resins in the SK water system was to prolong the life of the rather expensive CP resin. Since the quality of the SK water is quite high (resistivity is as high as 18.24 M$\Omega \cdot$m),

it is possible to remove ions only using CP resin for a reasonable time period without exchange. In October 2000, we have performed the following changes.

- Empty the IE two vessels and fill CP resin in the vessels.
- Empty the CP vessels.

We monitored the radon concentration changes before and after the water system improvement by using the three super high sensitivity radon detectors for water in real time. Figure 7.6 shows a typical variation before and after water system. These data points was monitored real-timely just before SK tank. The other monitoring points were just after IE system and just after UF system. The radon concentration after the water system improvement is shown by open circle in figure 7.3 and a numerical summary is shown in table 7.5.

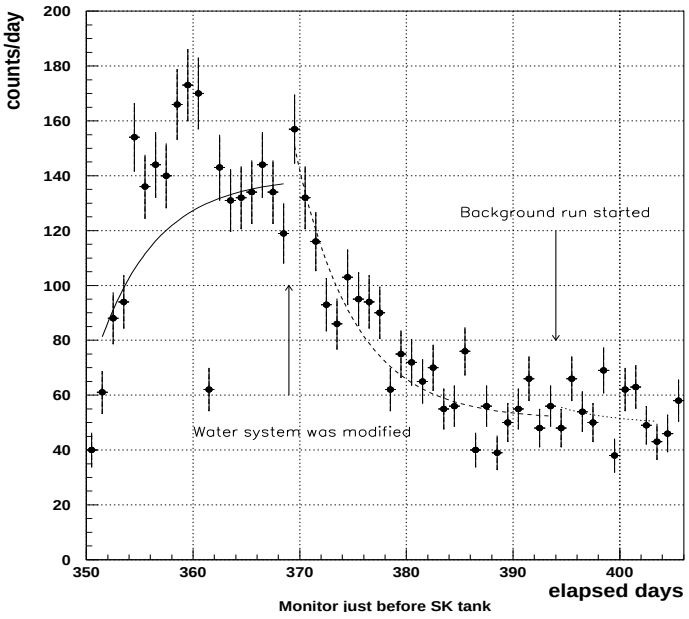

Figure 7.6: A typical variation before and after water system improvement in October 2000. These data was monitored real-timely just before SK tank.

Component	radon concentration before October improvement	radon concentration after October improvement
Just after IE	88.0±0.6	6.9±0.9
Just after UF	5.8±0.5	0.33±0.60
Just before the SK tank	6.5±0.2	0.96±0.74

Table 7.5: A comparison of the radon concentration between before and after the October 2000 improvement. Error is statistical only.

The radon concentration just after the IE vessel (now filled with CP resin) is decreased by more than a factor of 10. The detection of the limit in the radon detector for water is estimated 0.7 mBq/m^3/day in a one-day measurement. We did not observe clear excess of radon counts over the background level in the radon detectors at "Just after UF" and "Just before the SK tank" after the improvement. If the radon concentration in water is close to or lower than the equilibrium concentration with the background in a radon detector, no excess or negative excess should be observed. The radon concentration presented in table 7.5 is based on a simple

calculation done by subtracting the background counts. The background counts in the radon detector for water is measured in the state where the water flow through the detector is stopped.

In February 2001, the MD system was installed just before the SK tank in figure 3.16. We designed a system of 30 MD modules to process SK supply water of 30 tons/hour and to inlet the radon-free-air of 1.0 L/min to each module from the module test. Moreover, we covered the exhaust of a vacuum pump by the radon-free-air. The typical pressure in the MD system is 2.6 kPa. The typical concentration of the dissolved oxygen after the MD is 290 μg/L. In this setup condition, the removal efficiency for radon is supposed about 90%. However, we could not confirm the radon reduction efficiency for the low level radon achieved by the October 2000 improvement, because the module test was done in August 2000 and the radon concentration after the October 2000 improvement was low level which was not sensitive with the radon detector for water. We monitored the radon concentration of the SK supply water just before SK tank with the radon detector for water before and after MD system installation. We could not observe a change in the radon rates, therefore the radon concentration was kept less than 1.0 mBq/m^3 after MD system installation. But probably the radon reduction efficiency does not strongly depend on the initial radon concentration. By these improvements, we succeeded in radon reduction in SK supply water down to less than 0.7 mBq/m^3.

7.7 SK low-energy event rate

So far in this section, we have written about success in the radon reduction in the SK water supply. Hence, the SK detector is separated from radon rich environment. However this radon reduction does not make an effect on for reducing radon background for the solar neutrino analysis. Figure 7.7 shows a history the expected radon concentration in the SK tank from January 2000 to July 2001. One data plot indicates day or night data in a day.

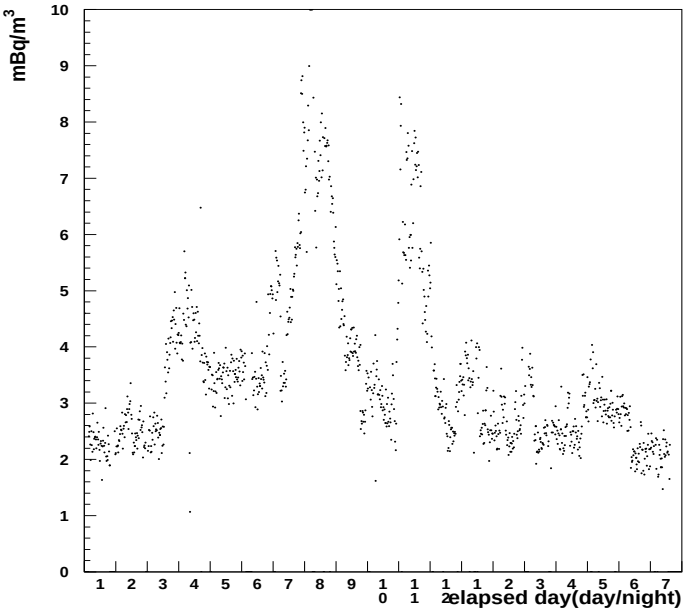

Figure 7.7: History of the expected radon concentration in SK tank calculated from the low-energy event rate between Jan. 2000 and Jul. 2001. One plot indicates radon concentration in day and night time.

The radon concentration is calculated from Super-Low-Energy event rates between 4.5 MeV and 6.5 MeV using the radon detection efficiency in the SK detector. The used events are within R<10 m, -16.1 m<Z<16.1 m (R:the radius axis of the SK tank, Z:the cylindrical axis of the SK tank). The event selection of R<10 m means that incoming gamma-ray events from the detector

wall are eliminated as far as possible. In order to estimate the radon concentration in the SK water independent of the radon detector measurements, we used the SK detector to take data with a known amount of radon in December 1997. The details were reported in reference [100]. From these test run, the radon detection efficiency is defined as a following equation :

$$0.013[\text{events/day/ton}] = 1.0[\text{mBq/m}^3] \tag{7.3}$$

This correlation factor was acquired by the analysis of Super-Low-Energy (SLE) events in this run at the hardware trigger threshold of -260 mV [94]. . The SLE events have energies between 4.5 MeV and 6.5 MeV. A fast vertex reconstruction and a fiducial volume cut (32 ktons) were applied to all the events in real-time on a workstation. After these cuts, the same event selections as the SK solar neutrino analysis are applied to SLE events for this analysis. Some additional noise cuts usually are also applied using the quality of the reconstructed vertex, but for the test run and the calculation of the radon concentration, the last cuts are not applied in order to leave the raw background events. The used events were within R<10 m, -16.1 m<Z<16.1 m.

Table 7.6 shows the radon detection efficiency in the SK detector for the another hardware trigger thresholds.

Run period	hardware trigger threshold	Radon detection efficiency for 1.0mBq/m^3
May. 1997∼	-260mV,-250mV	0.013[events/day/ton]
Sep. 1999∼	-222mV	0.015[events/day/ton]
Dec. 1999∼	-212mV	0.016[events/day/ton]
Sep. 2000∼	-186mV	0.022[events/day/ton]

Table 7.6: Radon detection efficiency in SK detector for another hardware trigger thresholds.

In the figure 7.7, the expected radon concentration in the SK tank was quite high in July∼August and November 2000. As described in last section, the radon concentration in the SK supply water is about 0.7 mBq/m^3 after October 2000 and February 20001 by the water system modification and MD system installation. However the radon concentration in the SK tank did not changed so much at 2∼3 mBq/m^3, except for the period of July∼August and November 2000. If the supplied water is uniformly diffused in the inner detector and the flow rate is 30 ton/hour, then the radon concentration at equilibrium is :

$$\frac{0.7[\text{mBq/m}^3] \cdot 720[\text{m}^3/\text{day}]}{0.182[1/\text{day}] \cdot 32000[\text{m}^3]} = 0.09[\text{mBq/m}^3] \tag{7.4}$$

The expected radon concentration in figure 7.7 is much higher than the contribution from the SK supply water. The large variations in the radon concentration of the SK tank in year 2000 is correlated with the changes of the SK supply water configuration. Table 7.7 summarizes the SK supply water configuration and the temperature of the SK supply water. figure 7.8 also shows a diagram of the SK supply water configuration.

The rise in the expected radon concentration in the SK tank in July∼August and November 2000 seems to be due to strong convection in the SK tank. Figure 7.9 shows the Z dependence of the water temperatures in the SK tank measured on August 22, 2000 and January 9,2001. The temperature measured on August 22, 2000 is uniform within 0.01 degree centigrade in the inner detector. On the other hand, the temperature profile on January 9 2001 shows that the water convection is caused only below Z=-10 m.

In this time, the radon concentration was kept at a low level. Figure 7.7 shows vertex position distribution of the low-energy data sample from 4.5 MeV to 6.5 MeV.

The event selection is the same as the stream of the radon detection efficiency. When the water temperature is not uniform, the distributions show that the radon background event rate

Date	Supply to	Return from	Supply water temperature
Before Mar.2000	bottom	top	∼12.3 degree centigrade
Mar.-Jul.2000	center	bottom	not measured
Jul.-Aug.2000	bottom	top	∼15.2 degree centigrade
Aug.-Oct.2000	bottom	top	∼14.3 degree centigrade
Oct.-Dec.2000	center	top(1/2)bottom(1/2)	∼14.3 degree centigrade
After Dec.2000	bottom	top	∼14.3 degree centigrade

Table 7.7: SK supply water configuration and temperature of SK supply water.

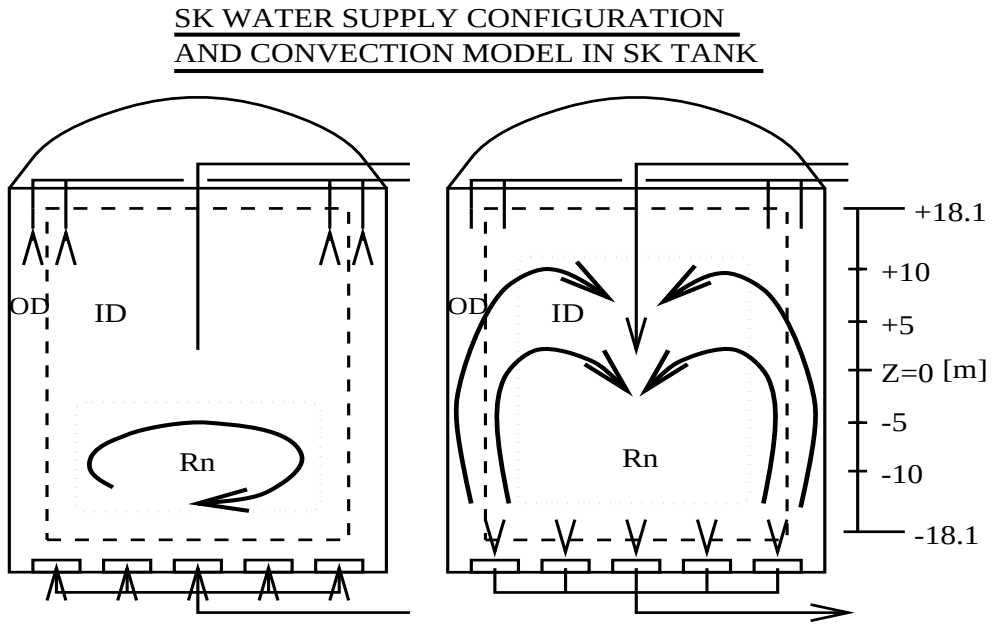

Figure 7.8: SK water supply configuration and convection model in SK tank. The left figure shows the small convection model when the SK water is supplied to bottom. The right figure shows the big convection model when the SK water is supplied to top.

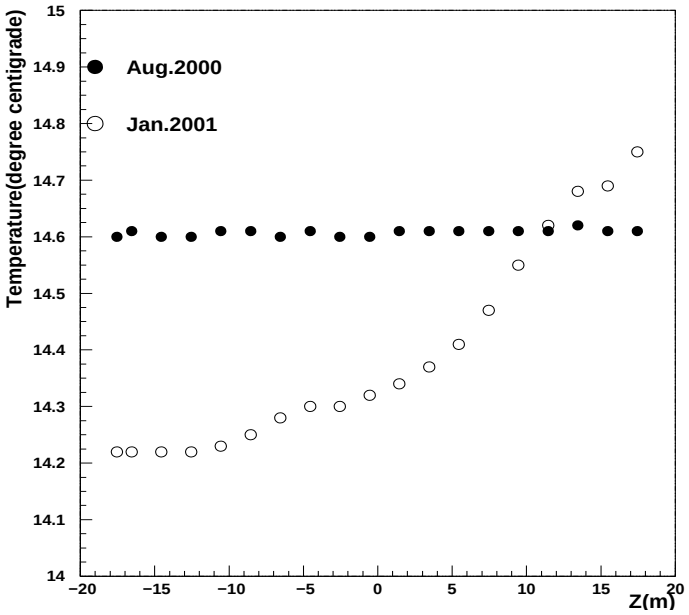

Figure 7.9: Z dependence of the SK water temperature measured on August 22 2000 and January 9 2001.

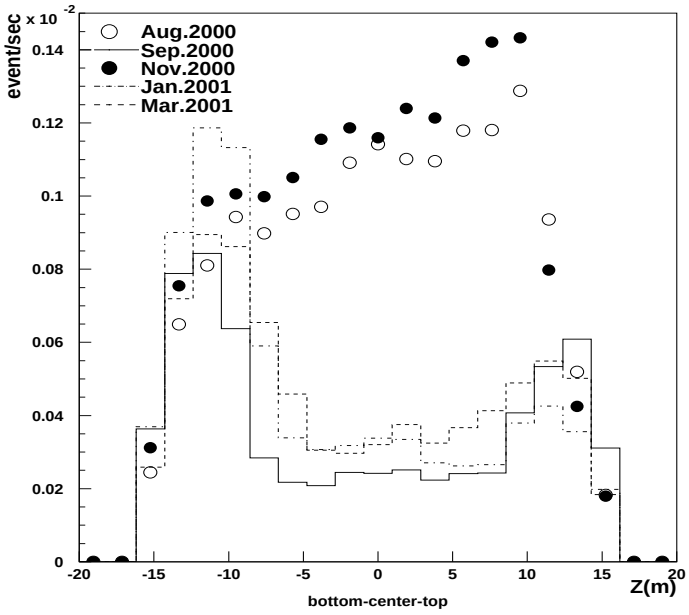

Figure 7.10: Z Vertex distribution of the low-energy events in Aug. 2000, Sep. 2000, Nov. 2000, Jan. 2001 and Mar. 2001.

is higher just in the bottom region of the SK tank and the radon concentration in figure 7.7 is low. On the other hand, when the water temperature is uniform, the distributions show that the radon background event rate is higher in the region where the water temperature is uniform and the radon concentration is high. Further, the integration of the distributions in the period when the water temperature is uniform is larger than another period when the water temperature is not uniform. Hence, we conclude that the emanation of radon from detector materials is the dominant source of radon, and the radon is transported by the convection in the SK tank. Figure 7.8 shows the our assumed convection model. The excess of vertex position distribution in the bottom region is caused by the model of the left plot in figure 7.8. The expansion of vertex position distribution in the convective period is caused by the model of the right plot in figure 7.8.

The radon emanation from various materials, namely PMTs, black plastic sheets and tyvek sheets, used in the SK tank in large quantities was measured. The measured PMTs are 20 inch PMTs used in the SK inner detector. The black plastic sheets and tyvek sheets are used in the inner and outer detector respectively. The measurement was performed by super-high sensitivity radon detector for air in which various materials were placed. The radon detector is reported about the details in reference [102]. Assuming that the radon emanated from each material is uniformly distributed over the whole SK detector (50 ktons), the equilibrium radon decay rate is given in the following equation. The 'Radon concentration in SK tank' indicates the results from the equation. Concerning the emanation from black sheets, the radon emanation is measured about the amount used around one PMT.

$$\frac{\text{Radon emanation}[\text{mBq/m}^2, \text{PMT/day}] \cdot 15000, 11146[\text{m}^2, \text{PMTs}]}{0.182[1/\text{day}] \cdot 50000[\text{m}^3]} = [\text{mBq/m}^3] \qquad (7.5)$$

The results is consistent with the expected radon concentration in the SK tank during large

Material	Radon emanation	Radon concentration in SK tank
Black sheet	0.08 mBq/PMT/day	0.10 mBq/m^3
Tyvek sheet	1.5 mBq/m^2/day	0.44 mBq/m^3
PMT	∼4.0 mBq/PMT/day	∼ 5.0 mBq/m^3

Table 7.8: Radon emanation from various materials.

convection periods (e.g. August and November 2000) within a factor of two.

As a next step, we confirmed whether the radon expected from SK low-energy event rate in the SK tank exists or not. We actually measured the radon concentration in the SK tank with the super-high sensitivity radon detector for water (700L radon detector) in May. 2001 when the radon concentration was low and it is assumed that the no large convection happened. Figure 7.11 shows a setup to measure Z dependence of the radon concentration in the SK tank.

The sample water is taken from each Z position, which are Z=+6.5 m (Center) and Z=-15.5 m (Bottom), via a rigid nylon tube with a water pump using the bypass route in the figure 7.11. Then the radon concentration of the sample water was obtained with the radon detector. The background level in the system was measured with the measurement of the radon less water made with 'Rn less making system' (See figure 7.11), which make use of the membrane degasifier module explained in the last section. The result in the measurement is the actual background level in this system. The detection limit of the radon detector is 0.7 mBq/m^3. Table 7.9 summarizes Z dependence of the radon concentration in the SK tank. Figure 7.12 also shows the same results.

We calculated the expected radon concentration in the bottom region from Z=-500 m to Z=-1610 m and the center region from Z=-500 m to Z=+500 m at R=0 using the SK low-energy event rate and the radon detection efficiency in May. 2001. The expected radon concentration is 4.1 mBq/m^3 and 0.0mBq/m^3 in the bottom and center region respectively. From these results,

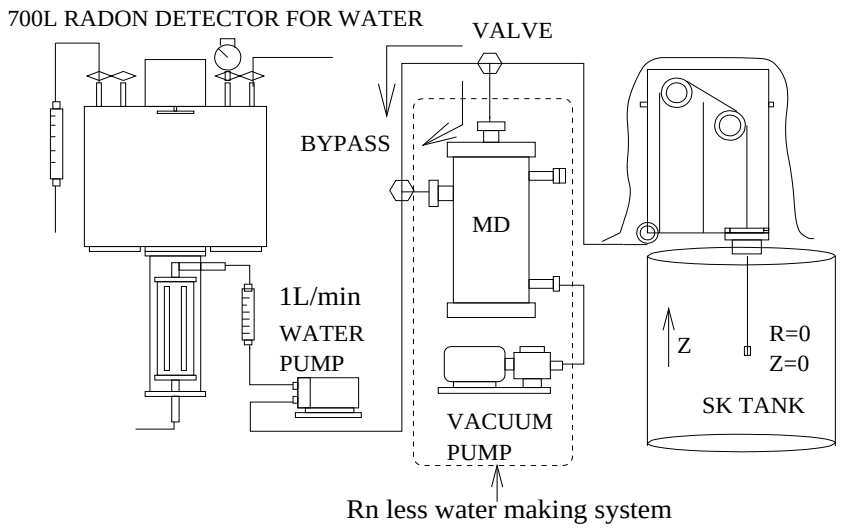

Figure 7.11: Setup to measure Z dependence of radon concentration in SK tank.

Position(R/Z)	Radon concentration	B.G subtraction
Rn less water(Actual B.G)	2.0±0.3mBq/m^3	-
Center(0.0/+6.5)	1.6±0.2mBq/m^3	<0.7 mBq/m^3
Bottom(0.0/-15.5)	3.2±0.2 mBq/m^3	1.6±0.5 mBq/m^3

Table 7.9: Z dependence of the radon concentration in SK tank.

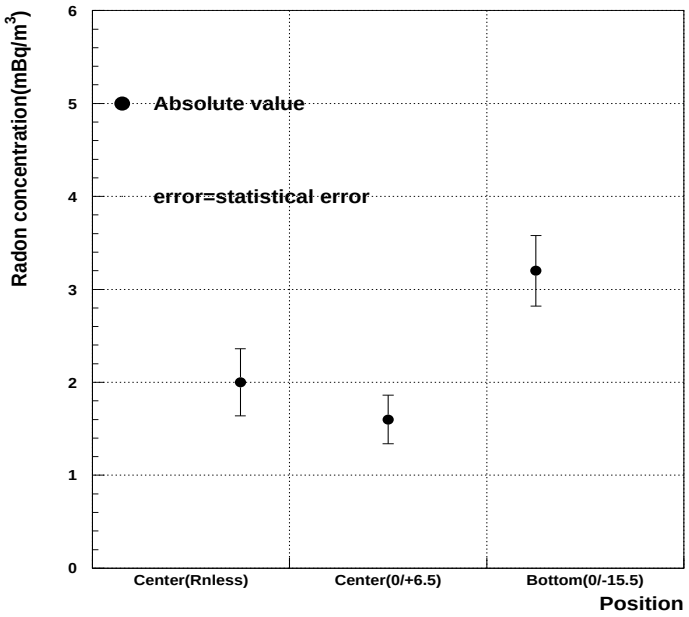

Figure 7.12: Z dependence of Radon concentration in SK tank.

we conclude that the radon concentration in the SK tank is not consistent with the expected value within a factor of 2.6, but we can confirm the radon existence in the bottom region of the SK tank in the small convection period. Moreover, when the large convection does not happen, the radon does not exist in the center region.

From the conclusions of the SK event rate analysis, we installed a new chiller system into the SK water purification system in March, 2000 in order to suppress the convection in the SK tank by lowering the SK supply water temperature to make the temperature gradient in the SK tank larger. Typical water temperatures before the 1st heat exchanger and after the 2nd heat exchanger are 14.5 degrees centigrade and 13.5 degrees centigrade, respectively in figure 3.16. The water temperature changed from 14.6 degree centigrades to 12.7 degree centigrades. However, we could not observe the effect of the installation in figure 7.7 clearly.

7.8 Summary

The radon concentration at various locations in the SK water purification system was measured. The radon source in the water system was investigated and improved in Dec 2000. The radon concentration in the SK supply water was decreased by a factor of about 5. We have also studied the feasibility of the Membrane Degasifier as the new radon reduction system in the water system. We found a optimum configuration of vacuum, water flow rate and radon-free-air flow rate. A system consisting of 30 Membrane Degasifier modules was installed in the SK water system in February 2001. By these improvements, the radon concentration in the SK supply water became less than 0.7 mBq/m^3 and the SK tank was separated from the external radon rich environment from a point of view of the radon background. After the water system improvements, the SK low-energy event rate was studied on the details. The SK event rate is much higher than the level expected from the supply water. It was concluded that the current main source of the radon background is the emanation from the PMT glass, and convection is the main driving force for transporting the radon in the detector. Even if radon moves from the surface of PMT to the inner of fiducial volume by Brownian motion, radon is able to move by about 10 cm [105]. The schematic view of estimated background contamination is like figure 7.13.

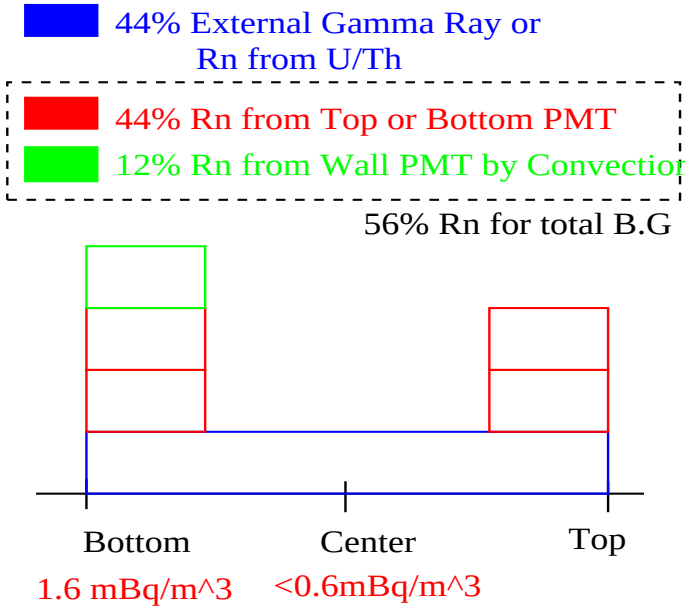

Figure 7.13: The schematic view the ratio of background contamination in SK detector.

7.9 Future prospects

Since the radon in the supplied water was reduced to a level acceptable for the solar neutrino analysis, we need to reduce the radon emanating from detector materials and to suppress the convection in the SK tank. We plan to do the following things for this purpose.

1. We changed the shape of the water outlet pipes in order to reduce the height of the convective zone as far as possible. We asked Mitsui-zosen Co. (SK tank company) to make a simulation program for the SK water flow. We found the optimized shape and length of the outlet pipes using the simulation. The improved pipes were replaced during the PMT replacement between July. 2001 and October. 2001 after SK-I. Figure 7.14 shows the improvement of the shape of the water outlet pipe. A new outlet pipe, which is made by transparent acrylic resin, was attached to the top of the old PVC outlet pipe. The new outlet pipe has many holes on the side of the pipe in order to let the water out in the horizontal direction.

2. We will measure radium concentration in SK tank water. As seen in the data of January. 2001 in figure 7.7, we still have background in the non-convective zone in the tank (continuum background from top to center). Is it due to radon produced from radium in water? We have installed RO system in March 2000 in order to increase the efficiency of removing radium. But, apparently the continuum background did not disappear. We need to measure radium in the SK water and understand the source of the continuum background.

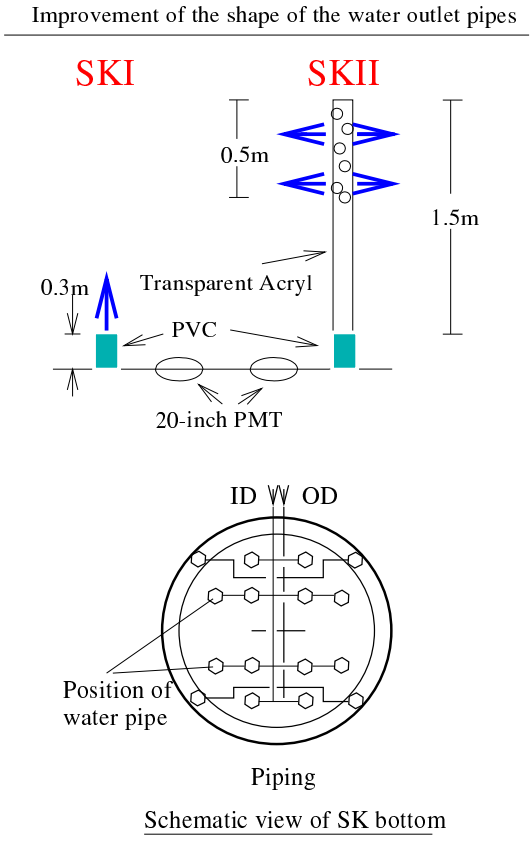

Figure 7.14: The improvement of SK water supply pipe to control water convection in SK tank.